Stochastic Analysis of Self-sustained Oscillation Loop for a Resonant Accelerometer

Chul Hyun*, Jang-Gyu Lee* , Taesam Kang** and Sang-Kyung Sung***

* Department of Electrical Engineering, Seoul National University, Seoul, Korea
(Tel : +82-2-880-7317; E-mail: hyun@asrignc3.snu.ac.kr)
**Department of Aerospace Engineering, Konkuk University, Seoul, Korea
(Tel : +82-2-450-3544; E-mail: tskang@konkuk.ac.kr)
***Telecommunication R&D Center, Samsung Electronics co., ltd. , Suwon, Korea
(Tel : +82-31-279-5839; E-mail: s.sung@samsung.com)

Abstract: In this paper, a nonlinear feedback system is analyzed for a surface micromachined resonant accelerometer. For this, a brief illustration of the plant dynamics is given. In the analysis, the periodic signal in the nonlinear feedback loop is obtained by the limit cycle point, which is best approximated via the describing function method. Considering the characteristic feature of plant dynamics, a simple phase shifted relay with finite slope is designed for the nonlinearity implementation. With a describing function for random plus sinusoidal input, we analyzed the effect of a white Gaussian noise on oscillation frequency. Finally, simulation and experimental result is given.

Keywords: Accelerometer, Resonant, Describing Function, Self-sustained oscillation loop

1. INTRODUCTION

An improved silicon micro accelerometer by surface micromachining technology is presented in this paper. The working principle of the differential type resonant accelerometer (DRXL) is just like conventional pendulous accelerometer and uses resonators to pick off the differential gap change induced by the applied acceleration. So it is less sensitive to the internal residual stress and the sensitivity to the acceleration can be doubled due to its differential characteristics. Furthermore, it uses surface micromachining processes which has been proven as a manufacturable technology. Thus the DRXL can be easily mass produce with low cost.

Mechanical part of the DRXL is machined by surface micromachining process. For a resonant sensor, high vacuum environment is realized by vacuum chip packaging. Signal processing parts have been implemented by hybrid electronic circuits.

Among these electronics, a closed loop system called self-sustained oscillation loop is prerequisite for its operation as a resonant accelerometer. A self-sustained oscillation loop induces the system's dynamic states into its primary mode, thus keeps track of its resonant state under applied acceleration or perturbation. For this, a simple self-sustained oscillation loop is designed and the feature of the loop is analyzed in the viewpoint of nonlinear dynamic system. The oscillation loop is regarded as a limit cycle. From the standpoint of feedback control system, both determination of resonance point and its stability analysis are required. For actual system which has several noise sources, these noise can affect the output resonant frequency.

The analysis has been done through the nonlinear system analysis methodology, describing function method and extended Nyquist criterion. Then by implementing the designed feedback loop, specifications of sensor performance could be obtained by various performance tests.

2. SENSOR STRUCTURE

2.1 Structure and operating principle

A resonance type accelerometer detects the variation of resonant frequency due to external acceleration. This type of accelerometer has some advantages of digital readout, wide output range and enhanced sensitivity over amplitude detection methods. Also capacitive pickoff is less sensitive to ambient temperature variation than piezo type or electromagnetic type methods. Thus we have used capacitive pickoff and frequency readout.

But this kind of parallel plate resonant structure has some drawbacks of non-linearity, and difficulty in controlling the resonant vibration mode within the stable region, because the vibrating mode is parallel to the input acceleration axis. In this paper, we decoupled the G-sensitive structure and gap sensitive resonator using separated torsion beams.

Fig.1 shows the simplified diagram of the one side inner resonator of the DRXL and illustrates principle of system operation

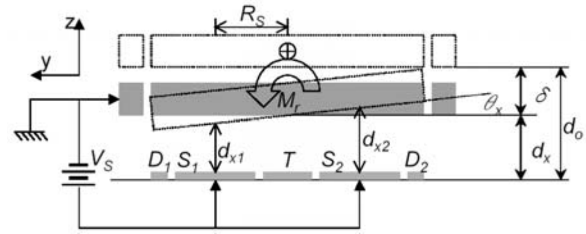

I_x : inertia
θ_x : tilt angle
R_S : distance of resonator - sensing electrode
V_S : applied bias voltage
d_x : gap distance
$D_{1,2}$: driving electrode
$S_{1,2}$: sensing electrode
T : tuning electrode

Fig. 1 Schematic for inner resonator.

Basic principle for resonance type accelerometer is to detect variation of resonant frequency due to the gap change between ceiling electrode (inertial mass) and bottom electrode (pickoff node) at the electrostatic actuator. When external acceleration is applied, a specific force moves outer gimbal in the direction of z. The resulting gap deviation from nominal states changes effective stiffness of the beam sustaining inertial mass differentially. Note that the electrostatic stiffness is a function of gap distance. Finally the variation of the effective stiffness induces variation in the vibrating frequency of the mass.

2.2 Plant dynamics

The governing equation for the system dynamics is modeled to be composed of mechanical and electrical part. Mechanical part says 2nd order dynamics which is composed of mass, damper and spring. Electrical part says electrostatic force induced by potential difference between electrodes. Equation (1) represents dynamic equation under specific force by external acceleration.

$$\tau_a = I_x\ddot{\theta}_x + D_x\dot{\theta}_x + k_{m_x}\theta_x - \tau_e \qquad (1)$$

where τ_a is the torque applied to the resonator and D_x, k_m and τ_e represent damping coefficient , mechanical stiffness of the resonator and electrostatic torque, respectively. If we differentiate electrical storage energy induced by potential difference between the electrodes, we can obtain effective electrostatic force in terms of system parameters. The effective torque applied to the resonator, τ_{eff_x} is given as the difference of the electrical torque from the applied mechanical torque.

$$\tau_{eff_x} = \tau_{m_x} - \tau_{e_x} = \theta_x \cdot k_{eff_x} = \theta_x \cdot \left(k_{m_x} - \frac{2R_S{}^2 \cdot \varepsilon \cdot A_S \cdot V_S{}^2}{d_x^3} \right) \qquad (2)$$

where ε and A_S represent dielectric constant and the area of the sensing electrode.

Then the resonance frequency is approximately given as

$$f_{rx} = \frac{1}{2\pi} \cdot \sqrt{\frac{k_{effx}}{I_x}} = \frac{1}{2\pi} \cdot \sqrt{\frac{1}{I_x}\left(k_{mx} - \frac{2R_S{}^2 \cdot \varepsilon \cdot A_S \cdot V_S{}^2}{d_x^3} \right)} \qquad (3)$$

Note that the effective stiffness (k_{effx}) of this electro-mechanically-biased resonator can be changed by the variable gap (d_x).

3. OSCILLATION LOOP ANALYSIS

Generally, feedback control systems can have nonlinear components in their loop. This frequently occurs because many practical control systems have saturation, relay and hysterisis by their physical constraints. In many of these cases, a periodic signal exists in the closed loop as a solution of the loop equation. In nonlinear control theory, this periodic signal is called limit cycle as a kind of equilibrium point. A useful approach in the analysis of the limit cycle is the describing function method. It can be used in determining the existence of limit cycle point and predicting its stability.

3.1 Sinusoid signal

In the case of resonant accelerometer, the vibrating signal of displacement in resonant mode can be taken as the very limit cycle. Thus an analysis about the limit cycle's existence and stability is quite necessary for the system's description. A procedure has been given for the limit cycle analysis of resonance type accelerometer.

The simplified block diagram of the nonlinear feedback system is given in the Fig. 2.

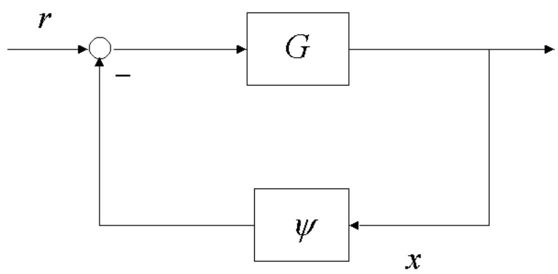

Fig. 2 Nonlinear feedback loop for DRXL.

The G(s) is the transfer function given by Eq. (1) and the ψ is the feedback nonlinearity that is inserted to keep resonant oscillation. And x represents the periodic signal, which practically becomes the displacement of mass.

Now the loop equation in Fig. 2 is given as

$$x = -G\psi(x) \qquad (4)$$

In the figure, let's first assume that the feedback system has symmetric and periodic solution. This is possible by defining the odd symmetric nonlinearity. Furthermore it can be shown that the periodic solution is half wave symmetric for the nonlinearity. Then, at the input of nonlinear component, periodic signal x can be represented as:

$$x(t) = a_1 \sin\omega t \quad (:= x_1(t)) + \sum_{k>1,odd}^{\infty} b_k \sin k\omega t \qquad (5)$$

where the right-hand side is sum of a dominant sinusoid denoted by $x_1(t)$ and its higher-order harmonics. Then the describing function technique simplifies the nonlinear loop equation in Eq. (4) into the first-order harmonic balance, namely

$$1 + G(j\omega)\psi_N(a_1)\, e^{j\phi} = 0 \qquad (6)$$

where $\psi_N(\cdot)$ denotes the describing function of $\psi(x)$ without the phase delay. To find an appropriate solution in (6), let's define the nonlinear feedback component. First an odd symmetric nonlinearity is designed for a real-valued describing function of a_1.

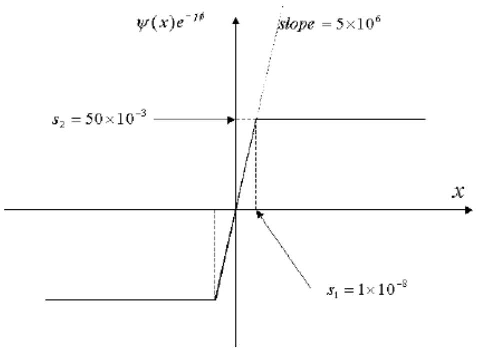

Fig. 3 Input-output relationship of feedback nonlinearity

Fig.3 shows the input-output relationship of the nonlinearity in the loop. Apparently finite slope of the relay is achieved to meet the real implementation problem. Also it plays an important role in the rigorous proof of existence problem. With some calculation, we can find the describing function for the nonlinearity as (7).

$$\psi_N(a_1) = \frac{2\times(c_2 - c_1)}{\pi}\left[\sin^{-1}\left(\frac{s_1}{a_1}\right) + \frac{s_1}{a_1}\sqrt{1-\left(\frac{s_1}{a_1}\right)^2}\right] \tag{7}$$

In equation (7), c_1 and c_2 is the boundary slope of the nonlinearity. Note that the determined a_1 becomes the amplitude of the limit cycle which is obtained from the determining equation (6). But just from the functions of plant linear model and (7), the limit cycle point cannot satisfy the resonant frequency near plant dynamics. Thus to get a near frequency solution, a phase difference between the nonlinearity is necessary. By including the phase shifter in the nonlinear feedback loop, the modified describing function is represented as,

$$\Psi_N(a_1,\phi) = \psi_N(a_1)e^{j\phi} \tag{8}$$

Through the representation of the describing function and the plant dynamics model, an equation for the limit cycle can be represented form (6) and (8).

$$G(j\omega) + \frac{1}{\Psi_N(a_1,\phi)} = 0 \tag{9}$$

The solution a_1 and ω for equation (9) determine the trajectory of limit cycle, that is, the amplitude and frequency. Figure 4 shows the above arguments graphically in terms of describing function and plant model. In the figure, two loci are given; one is for Nyquist plot representing plant dynamics and the other for describing function in the complex plane. The intersection point of these two loci is the point where the 1st order harmonic balance equation holds. So we can determine the limit cycle point by choosing an appropriate magnitude of oscillation, a_1.

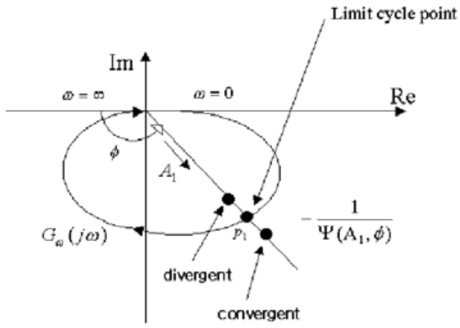

Fig. 4 Determination and stability of self oscillation

A quasi-static stability of the self-sustained oscillation can be investigated by means of the extended Nyquist stability criterion. With the help of this classical tool, since points near the intersection and along the a_1-increasing side, are not encircled by the plant's loci, the determined operating point is stable. This quasi-static stability analysis is quite important for practical implementation. Also, the stability robustness of the limit cycle may be taken effect on by the structure of the neglected higher order terms, but the low pass property of the loop fairly lessens the effect of high frequency component.

3.2 Sinusoidal and white Gaussian noise signal

Actual system has several noise sources. Mechanical thermal noise, electrical thermal noise, shot noise, 1/f noise and so on. So analysis of the effect of random noise input, which is applied when limit cycle induced in the system, is meaningful. Throughout the remainder of the paper the random signal is assumed to be Gaussian. This assumption is reasonable by the low pass property of a linear plant.

In this case, we are consider a describing function for random plus sinusoidal input : RSDF. In the presence of Gaussian distribution $(0,\sigma^2)$ noise, block diagram of the nonlinear feedback system is given in the Fig. 5. It has approximated optimal gains ψ_S and ψ_w for the sinusoidal signal and white Gaussian signal, respectively. And x represents the periodic signal with Gaussian noise.

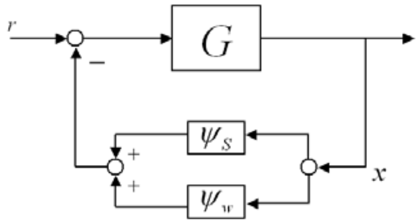

Fig. 5 Block diagram for sinusoidal and white noise

From the modified nonlinearity approach, we can obtain the components of the RSDF, $\psi_S(a,\sigma)$ and $\psi_w(a,\sigma)$.

$$\begin{aligned}\psi_S(a,\sigma) &= \frac{2\alpha_{10}}{a}\\ \psi_w(a,\sigma) &= \alpha_{01}\end{aligned} \tag{11}$$

$$\alpha_{sk} = \frac{1}{2\pi}\int_{-\infty}^{\infty} N(j\omega)e^{-\sigma^2\omega^2/2}(j\omega)^k j^s J_S(a\omega)d\omega \tag{12}$$

where $N(j\omega)$ is the Fourier transform of nonlinearity and J_s is the Bessel function of order s.

For the nonlinearity as previously defined (Fig. 3)

$$\begin{aligned}\psi_S(a,\sigma)&=\frac{s_2}{s_1}\sum_{n=0}^{\infty}\left(\frac{\sqrt{2}\delta}{\sigma}\right)^{2n+1}\frac{\Gamma(n+1/2)\,{}_1F_1(n+1/2;2;-\rho^2)}{(2n+1)!}\\ \psi_w(a,\sigma)&=\frac{s_2}{s_1}\sum_{n=0}^{\infty}\left(\frac{\sqrt{2}\delta}{\sigma}\right)^{2n+1}\frac{\Gamma(n+1/2)\,{}_1F_1(n+1/2;1;-\rho^2)}{(2n+1)!}\end{aligned} \tag{13}$$

where $\rho=a/\sigma\sqrt{2}$ is the signal to noise ratio, and ${}_1F_1(\alpha;\gamma;x)$ is the confluent hypergeometric function defined by

$${}_1F_1(\alpha;\gamma;x)=1+\frac{\alpha x}{\gamma}+\frac{\alpha(\alpha+1)}{\gamma(\gamma+1)}\frac{x^2}{2!}+\cdots \tag{14}$$

With these equations, it is difficult to obtain the analytic solution or graphical analysis result as previous case. So we have analyzed this case by numerical method and computer simulation.

4. SIMULATION AND EXPERIMENT RESULTS

4.1 Simulation

For a more precise interpretation of the system's behavior, a computer simulation using Simulink is given. The nonlinear plant model is constituted. We can obtain the value of inner resonator by solving nonlinear differential equation numerically.

Applied white Gaussian noise are showed in Fig. 6. At 0.04sec and at 0.06sec, 1×10^{-4} and 1×10^{-2} standard deviation white noise are applied respectively.

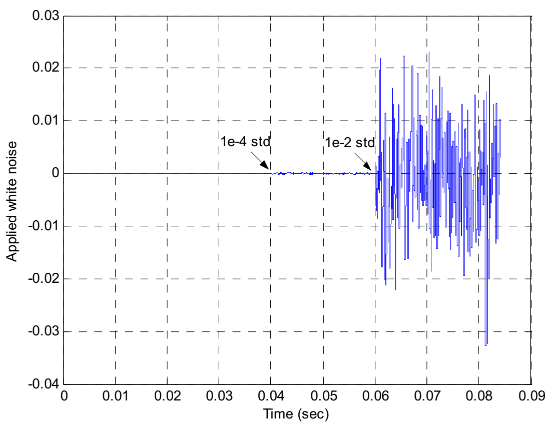

Fig. 6 Applied white Gaussian noise

Under noisy condition, output frequency of resonator has been perturbed. Fig. 7 shows the perturbation of output frequency due to applied white Gaussian noise.

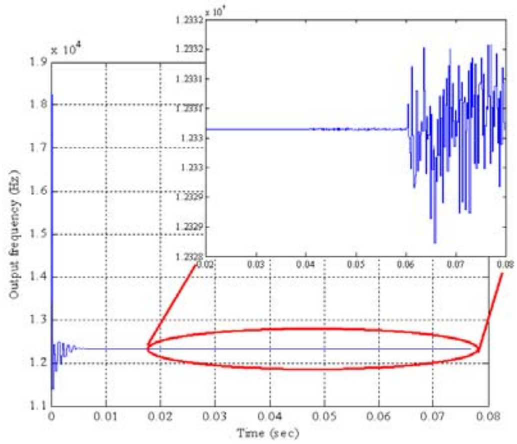

Fig. 7 Output frequency of the resonator

Fig.8 shows the displacement of resonator. We can see that the resonator oscillates sinusoidally.

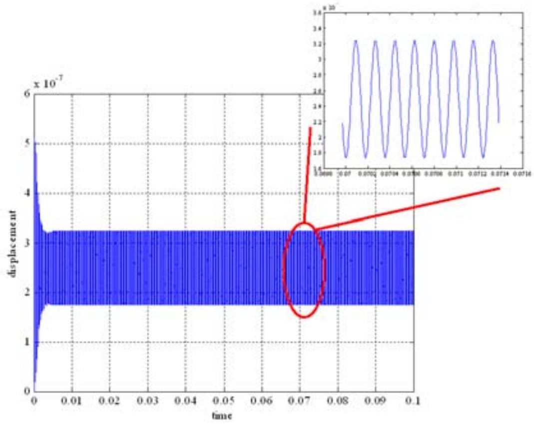

Fig. 8 Displacement of resonator

From the simulation, the proportional relation of input white noise and output frequency deviation is obtained. It is ploted in Fig. 9.

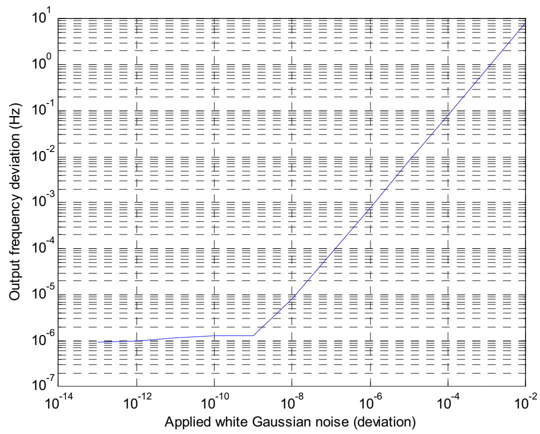

Fig. 9 Input noise – output frequency deviation

4.2 Experiment result

With packaged DRXL chip and signal processing electronics we have done several test. Fig. 10 shows the resonant characteristic of the DRXL. In the Fig. 10(a), it can be seen that the nominal resonant frequency is about 12.532kHz, signal to noise ratio (SNR) is about 25dB, and the quality factor is about 250.

When the phase and gain of the feedback components are fixed, the oscillation loop activates a resonance with the help of initial white noise in the driving voltage. The settling time to resonance is less than 30 ms, as shown in Fig. 8.

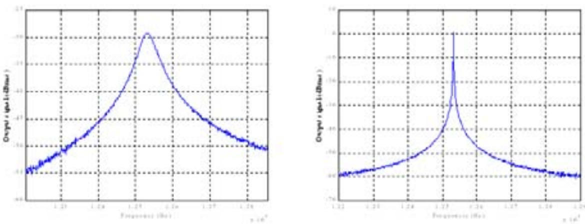

(a) resonator only (b) with self-oscillation loop

Fig. 10 Resonance characteristic of DRXL

Fig. 10 (b) shows an output of the designed loop in the frequency domain. From Fig. 10 (b), a *Q*-factor of 40000 is obtained, which shows quite an improved resolution compared to that of the sensing device only.

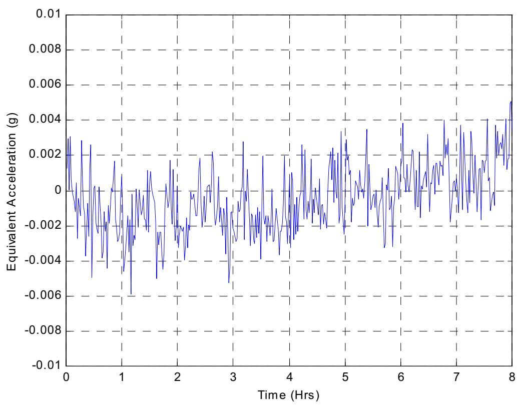

Fig. 11 Output frequency of DRXL (0 input)

Fig. 11 shows the static bias drift of the DRXL when zero gravity is applied. The obtained equivalent bias drift is about 2 mg of 1 σ standard deviation from output data for 10 hours. It is equivalent to a output frequency deviation about 14mHz.

5. CONCLUSION

A nonlinear feedback loop for the micromachined resonant accelerometer system is presented. And a brief illustration of the plant dynamics is given. The implementation of a resonant system is possible via a kind of nonlinear feedback system called self-sustained oscillation loop. A theoretic analysis is done for the nonlinear loop. In the analysis, the describing function method is used for the determination of the limit cycle. And the determined limit cycle point predicts the magnitude and frequency of the sinusoid in the loop. Some graphical illustration is given for an insightful interpretation. And the effect of a white Gaussian noise on oscillation frequency is analyzed. Finally, simulation and experimental result is given.

ACKNOWLEDGMENTS

This work is supported by Automatic Control Research Center in SNU and Brain Korea 21 program.

REFERENCES

[1] D. P. Atherton, "Nonlinear control engineering", *Van Nostrand Reinhold Company Ltd.*, 1975

[2] A. Gelb and W.E. Vander Velde, "Multi-input describing functions and nonlinear systems design", *New York: McGraw-Hill*, 1968

[3] B. L. Lee, C. H. Oh, Y. S. Oh and K. Chun, "A novel resonant accelerometer; variable electrostatic stiffness type," *Proceedings of International Conference on Solid State Sensors and Actuators*, 1999, Sendai, pp.1546-1549.

[4] L. Lee, C. H. Oh, S. Lee, Y. S. Oh and K. Chun, "A vacuum packaged differential resonant accelerometer using gap sensitive electrostatic stiffness changing effect," *Proceedings of the 13th International Conference on MEMS*, January 2000, Miyazaci, pp.352 –357.

[5] S. Sung, J. G. Lee, T. Kang and J. W. Song, "Design and analysis of nonlinear feedback loop for a resonant accelerometer," *Proceedings of European Control Conference (ECC 2001),* September 2001, Porto, pp.1906-1911.

[6] M. A. Meldrum, "Application of vibration beam technology to digital acceleration measurement," *Sensor and Actuators*, Vol. A21-A23, 1990, pp377-380.

[7] T. V. Rozhart, et al., "An inertial-grade, micromachined vibrating beam accelerometer," *Eighth International Conference on Solid-State Transducers and Actuators (Transducers `95)*, 1995, pp.659-662.

[8] S. Sung, *A Feedback Loop Design for MEMS Resonant Accelerometer Using a Describing Function Technique*, Ph.D. Thesis, Seoul National University, Feb 2003.